



ELSEVIER

Journal of Chromatography A, 918 (2001) 25–36

JOURNAL OF
CHROMATOGRAPHY A

www.elsevier.com/locate/chroma

Liquid-core waveguide technology for coupling column liquid chromatography and Raman spectroscopy[☆]

Reyer J. Dijkstra, Cees J. Slooten, Aike Stortelder, Joost B. Buijs, Freek Ariese,
Udo A. Th. Brinkman, Cees Gooijer*

*Department of Analytical Chemistry and Applied Spectroscopy, Division of Chemistry, Free University Amsterdam, De Boelelaan 1083,
1081 HV Amsterdam, Netherlands*

Received 20 November 2000; received in revised form 13 February 2001; accepted 26 February 2001

Abstract

The on-line coupling of liquid chromatography (LC) and Raman spectroscopy (RS) via an entirely plastic liquid-core waveguide (LCW) was optimized in terms of excitation wavelength of the laser, especially in relation to the fluorescence background, and the length of the LCW. Excitation at 632.8 nm (He–Ne laser) was found to be a good compromise between a wavelength long enough to strongly reduce the fluorescence background and, on the other hand, short enough to avoid (re)-absorption of laser light and Raman signals by H₂O in LCWs of considerable length. This conclusion is supported by a theoretical discussion on the optimization of LCW lengths as function of the excitation wavelength for H₂O and ²H₂O. When using the He–Ne laser the optimum length is ~50 cm for H₂O; this corresponds to a detection cell volume of 19 μl for an LCW of 220 μm I.D., which is fully compatible with conventional-size LC. The influence of an organic modifier, usually necessary for reversed-phase LC, on the free spectral window was evaluated. The potential applicability of LC–LCW–RS was shown for a mixture of adenosine 5′-monophosphate (AMP), guanosine 5′-monophosphate (GMP) and uridine 5′-monophosphate (UMP), utilizing an aqueous eluent without the addition of a modifier. Improved detectability was achieved by using the stopped-flow mode and applying a large-volume-injection procedure (injection volume: 200 μl). Under these conditions, the limit of identification for AMP, GMP and UMP was in the 0.1–0.5-mg/ml range. © 2001 Elsevier Science B.V. All rights reserved.

Keywords: Raman spectroscopy; Liquid-core waveguide; Detection, LC; Nucleoside phosphates

1. Introduction

Raman spectroscopy (RS) is a powerful analytical

tool, which provides detailed vibrational information as does Fourier transform infrared (FT-IR) spectroscopy, and therefore has a high analyte identification potential. In contrast to FT-IR it can easily be used for aqueous solutions, and is therefore suitable for biological samples. However, RS suffers from an extremely low sensitivity.

In order to improve the low sensitivity, the use of detector cells with increased optical pathlength was proposed three decades ago [1]. For this purpose

[☆]Presented at the 29th Scientific Meeting of the Spanish Group of Chromatography and Related Techniques, Alcalá de Henares, Madrid, 12–14 July, 2000.

*Corresponding author. Fax: +31-20-4447-543.

E-mail address: goojer@chem.vu.nl (C. Gooijer).

various types of liquid-core waveguides (LCWs) have been considered: if the refractive index (RI) of the capillary material is lower than that of the core liquid, excitation or Raman light that hits the capillary wall under an angle equal to, or larger than the critical angle to the normal will be captured inside the capillary. Four types of LCW can be distinguished: (i) internally, or externally metal-coated tubing, (ii) uncoated glass tubes, (iii) internally or externally plastic-coated tubes and (iv) entirely plastic tubes [2]. Although metal-coated LCWs can increase the optical pathlength and have the advantage of guiding light through virtually any transparent liquid, regardless of its RI, the approach suffers from high attenuation. As regards the uncoated glass tube LCWs, here light is reflected at the outer glass/air interface rather than at the liquid/glass interface. As a consequence, the light guiding is independent of the RI of the liquid. However, such LCWs are very fragile, and the loss characteristics are largely dependent on the outer glass surface. Therefore, much care has to be taken to create and maintain a clean and smooth surface. LCWs internally or externally coated with a plastic material have the advantage that they are more robust than the uncoated glass tubes. However, most plastics have an RI larger than that of water. A few years ago, Altkorn et al. [2] reported losses of ~ 1 dB/m over much of the visible spectral range for a water-filled capillary of fused-silica externally coated with Teflon AF2400, a clear amorphous perfluoropolymer having an RI of 1.29. Although the transmission properties were very favorable, the capillary is still quite fragile and has the disadvantage associated with light propagation in the silica wall. Recently, a breakthrough has been achieved: an LCW has been constructed made entirely of Teflon AF2400, which eliminates most of the earlier mentioned problems [3]. Compared to measurements performed in a standard 1-cm cuvette, an enhancement factor of ~ 20 for water and ~ 120 for benzene with a 1-m long LCW was reported, using a diode laser with an emission wavelength of 785 nm [4].

The new technology opens perspectives to improve the limits of detection (LODs) in various optical techniques to be coupled with liquid-based separation methods. Gooijer et al. [5] demonstrated

the use of a Teflon AF2400 LCW for improving LODs in conventional-size column liquid chromatography (LC) coupled with absorption detection by 30–50-fold. Holtz et al. [6] used an LCW to create a small-volume Raman detector, in which transverse illumination was used and end-on detection through a transparent window at the tube terminus. Dijkstra et al. [7] coupled conventional-size reversed-phase LC (RPLC) and RS using an LCW with a length of 30 cm and an I.D. of 280 μm . Three-dimensional chromatograms were recorded, showing on-the-fly Raman spectra for a test mixture of four nitro compounds. An LOD of 10 $\mu\text{g/ml}$ was obtained for 4-nitroaniline, a detection limit that is partly ascribed to on-column analyte preconcentration. Marquardt et al. [8] coupled microbore LC and RS. A total of ten structurally related alcohols were separated without the use of an organic modifier and LODs in the $\mu\text{g/ml}$ range were reported. Although the LODs in LC–RS are still rather high, the combination of the two techniques looks promising. The research is in an exploratory stage and much optimization still has to be done. In addition, there are alternative approaches to improve the sensitivity of RS; these are based on resonance and/or surface-enhanced effects. Until now, the on-line coupling of LC and resonance RS hardly received attention in the literature; we are aware of only one preliminary study reported in 1992 [9]. Surface-enhanced (resonance) Raman spectroscopy has been successfully coupled to LC in the at-line mode, i.e. after analyte deposition on a substrate [10–12]; its on-line coupling has been reported as well [13]. It should be realized however that the development of LC–RS has some distinct advantages: only a fraction of the vibrations which are active in RS are observed in the resonance and surface-enhanced modes.

In this paper we further explore the characteristics of LCWs with emphasis on the on-line coupling to LC. First of all the use of organic modifiers will be evaluated. Then the accent is on the light transmission of the LCW, the role of the fluorescence background, and the optimization of excitation wavelength and LCW dimensions. Finally, as a demonstration of the potential applicability of LC–LCW–RS, the separation and identification of three nucleotides are presented.

2. Experimental

2.1. LC system

The LC system consisted of a Separations Model 300 CS pump (H.I. Ambacht, Netherlands) with a laboratory-made six-port injection valve. Unless stated otherwise, stopped-flow experiments were performed, the flow being stopped a predetermined delay time after injection. The eluent was water and the flow 0.7 ml/min.

For the column liquid chromatography experiments, a 150×3 mm I.D., 5- μm Inertsil ODS-2 column (Chrompack, Bergen op Zoom, Netherlands) and a Kratos Analytical (Ramsey, NJ, USA) Spectroflow Model 757 absorbance detector were fitted. After the absorbance detector the effluent was led to the LCW interface. The eluent was aqueous 100 mM phosphate buffer, pH 6.0, and the flow 0.4 ml/min. Stopped-flow experiments were performed by switching a laboratory-made six-port valve between UV detector and LCW, a predetermined delay time after the analyte was monitored by the UV detector. This allows recording over an extended period of time. An injection volume of 25- or 200- μl was used. Standard injections were diluted in water; large volume injection in aqueous 100 mM phosphate buffer, pH 2.0.

2.2. Chemicals

HPLC-grade water was obtained from J.T. Baker (Deventer, Netherlands), deuterium oxide (99.8 at. % ^2H) from Janssen (Geel, Belgium) and sodium dihydrogen phosphate monohydrate (p.a.) from Merck (Darmstadt, Germany). 4-Nitroaniline, adenosine 5'-monophosphate (AMP) disodium salt, guanosine 5'-monophosphate disodium salt (GMP) and uridine 5'-monophosphate disodium salt (UMP) were from Fluka (Buchs, Switzerland). L-Phenylalanine and DL-serine were from Sigma (St. Louis, MO, USA).

2.3. Detection system

The LC–LCW–RS system described before [7]

was used with minor modifications; a brief description will therefore suffice. The LCW consisted of Teflon AF2400 and had an O.D. of 806 μm and an I.D. of 223 μm (Random Technologies, San Francisco, CA, USA). Unless stated otherwise, an LCW with a length of 50 cm was used. Interfacing of the LCW with the laser light was achieved by using two laboratory made poly(ethylene terephthalate) termination heads. In each of these, two holes were drilled and provided with a Valco thread. A tiny eluent chamber was formed between these holes, which was sealed by a quartz window. The LCW was fixed inside the termination head by means of a fingertight.

The light of a He–Ne laser (632.8 nm, 32 mW; Model 107S, Spectra-Physics, Mountain View, CA, USA) or an argon ion laser (514.5 nm, power up to 2 W; Innova 100, Coherent, Palo Alto, CA, USA) was transmitted through a bandpass filter to reduce the non-lasing emission and coupled into the LCW by a lens ($f=100$ mm). The Raman scattering was collected in the “forward mode”. A collimating lens ($f=50$ mm) and a focusing lens ($f=160$ mm) were used to couple the LCW output into a single-stage spectrograph (Monospec 18, Scientific Measurement Systems, Grand Junction, CO, USA). In front of the spectrograph was a holographic super notch filter (HSNF-633-xx or HSFN-514-xx, Kaiser Optical Systems, Ann Arbor, MI, USA) to remove the laser light. The spectrograph had a focal length of 156 mm, a grating of 1200 lines/mm and a slit width of 200 μm , which resulted in a spectroscopic resolution (FWHM) of 21 cm^{-1} . The Raman spectra were recorded with a cooled (-40°C) Andor Technology Model DV420-OE CCD camera (Belfast, UK). The spectrograph was calibrated by filling the LCW with acetonitrile–methanol (1:1, v/v), and assigning the vibrational bands according to the NIST library [14].

In principle, the Raman scattering can be collected in the “forward” or “backward” configuration. It has been pointed out in the literature that the latter configuration will have a 17% stronger signal at the optimum LCW length [1]. However, in the forward mode the experimental set-up is less complex, because the laser light is coupled into the LCW on one end and the Raman signal is collected on the other. For this reason we performed our experiments in the forward mode.

The experiments described in “Optimization of excitation wavelength and LCW length”, were performed with a slightly different set-up; a He–Ne laser of 15 mW was used (Nippon Electric, Tokyo, Japan) and the Raman spectra were recorded with a cooled Princeton Applied Research intensified (Princeton, NJ, USA) linear photodiode array detector and an EG&G OMA III Series Model 1460 optical multichannel analyzer.

3. Results and discussion

3.1. Organic modifiers

In a previous paper we studied on-line RPLC–LCW-RS for the separation of four nitro compounds (NO_2 vibrations, $1300\text{--}1346\text{ cm}^{-1}$) using aqueous methanol as the eluent [7]. Obviously, the use of this organic modifier adversely affected the analyte identification by means of RS, because vibration bands of methanol interfered with the NO_2 vibration of the analytes. Replacing methanol by modifiers such as acetonitrile or acetone did not result in a free

spectral window for the NO_2 vibration (Fig. 1). On the other hand, pure water is a very weak Raman scatterer and offers a large free spectral window for analyte identification. These observations imply that LC–LCW-RS will have prospects especially for separation systems that use aqueous eluents without added organic modifiers, e.g. ion-exchange and size-exclusion LC applied to biopolymeric compounds. In all subsequent experiments purely aqueous eluents were used.

3.2. Transmission experiments

Obviously, the attenuation of light through the LCW should be as small as possible. For practical use, we prefer to use transmission in percent rather than attenuation in dB/m (notice that an attenuation $>10\text{ dB/m}$ (or a transmission $<10\%$ for a 1-m capillary) will be useless for a Raman detector in the “forward mode”). The transmission of the LCW is determined by calculating the ratio of the signal of an amplified photodiode before and after the LCW. This transmission was typically 40% for a 50-cm long LCW. This value was not corrected for light

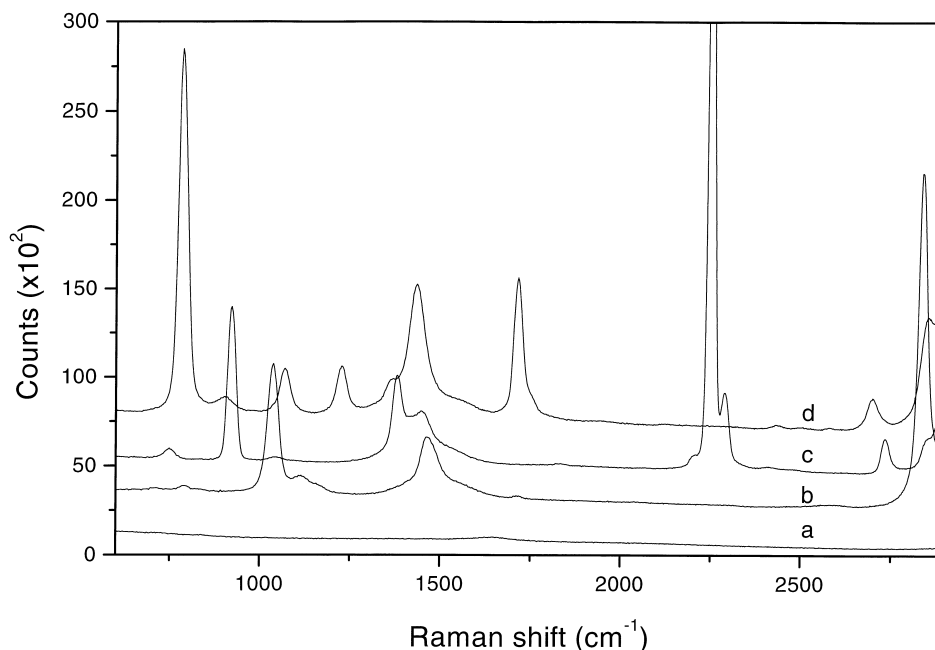


Fig. 1. Raman spectra of various solvents; (a) water, (b) methanol, (c) acetonitrile and (d) acetone. Excitation wavelength: 632.8 nm. Exposure time: 50 ms.

losses caused by coupling the light into the LCW. We observed that the position and, surprisingly, the angle of the LCW relative to the laser beam are very critical parameters. Before starting our experiments, the transmission of the LCW was optimized daily by means of an x - y - z translation table.

In general, the transmission of light through the LCW was constant during an 8-h working day. However, one has to be aware of memory effects: it was observed for instance that the transmission of the system rapidly diminished when the LCW was filled with an aqueous solution of 0.5 mg/ml 4-nitroaniline, a test compound. Subsequent flushing for 30 min with water resulted in a slow increase of the transmission. Flushing with 1 M KOH was, however, much more efficient. Teflon 2400AF is known to be very permeable to many compounds in the gas phase; hence analyte molecules present in the solution can easily penetrate and dissolve in the Teflon AF2400 wall. Obviously, care has to be taken to prevent memory effects. For similar reasons, Song et al. [4] used flushing steps with acetone, methanol and deionized water.

3.3. Background fluorescence

A major problem in LC-RS is the background fluorescence, which easily masks the weak Raman signals. This broadbanded fluorescence covers most of the visible region of the spectrum and reaches a maximum near the center of the visible region. There are two approaches to minimize this background: switching the excitation wavelength either to the deep-UV region (as was demonstrated by Asher and Johnson [15]) or to the (near)-IR region. In the latter region only very few compounds show strong absorption and cause fluorescence. Another interesting approach is to discriminate the Raman and fluorescence signals in time, since Raman has a lifetime of typical 10^{-14} s and fluorescence of 10^{-8} s. However, this requires a fast gatable detector and a pulsed laser system.

In our experiments, at an excitation wavelength of 514.5 nm a high background signal was observed: when using an LCW filled with water, a broad fluorescence band between 1000 and 2500 cm^{-1} appeared; its origin is unknown. This fluorescence signal slowly decreased in time (photo-bleaching),

but increased again when fresh water was put into the LCW. Altkorn et al. [16] observed similar background problems at an excitation wavelength of 532 nm. Shifting to the excitation wavelength of 632.8 nm of a He-Ne laser largely circumvents this problem. In Fig. 2 the Raman spectra of 10-mg/ml solutions of phenylalanine, DL-serine and UMP in water are shown, recorded at excitation wavelengths of 514.5 and 632.8 nm in stopped-flow experiments. The laser light intensity of the argon ion laser was reduced to 28 mW (by means of a variable beam-splitter) which is comparable to that of the He-Ne laser. Although the spectra are background corrected for the contribution of water, there is a steep slope for the spectra recorded at 514.5 nm, which is due to the fluorescence background. Obviously, the Raman spectra recorded at 632.8 nm are to be preferred. Further experiments were, therefore, performed with an excitation wavelength of 632.8 nm.

3.4. Optimization of excitation wavelength and LCW length

Walrafen et al. [1] derived an equation for the Raman signal as a function of the LCW length for the forward collection mode:

$$dI_R = CI \cdot dx - \alpha_R I_R \cdot dx \quad (1)$$

where I_R is the Raman intensity, C a constant related to the optical geometry, the analyte concentration and the Raman cross-section, I the laser intensity and α_R the loss coefficient at the Raman scatter wavelength. If, for convenience, it is assumed that the loss coefficients for λ_{ex} (the excitation wavelength) and λ_{Raman} (the Raman scatter wavelength) are identical so that $\alpha_L = \alpha_R$, I_R can be written as:

$$I_R = CI_0 L e^{-\alpha_L L} \quad (2)$$

where L is the LCW length (Appendix A). To find the optimum LCW length, S , the derivative of Eq. (2) has to be set equal to zero. Thus, S is given by:

$$S = \frac{1}{\alpha_L} \quad (3)$$

Unfortunately, in RS the above approximation is too crude. In an aqueous solution the absorption of laser light and Raman scattering by the overtone

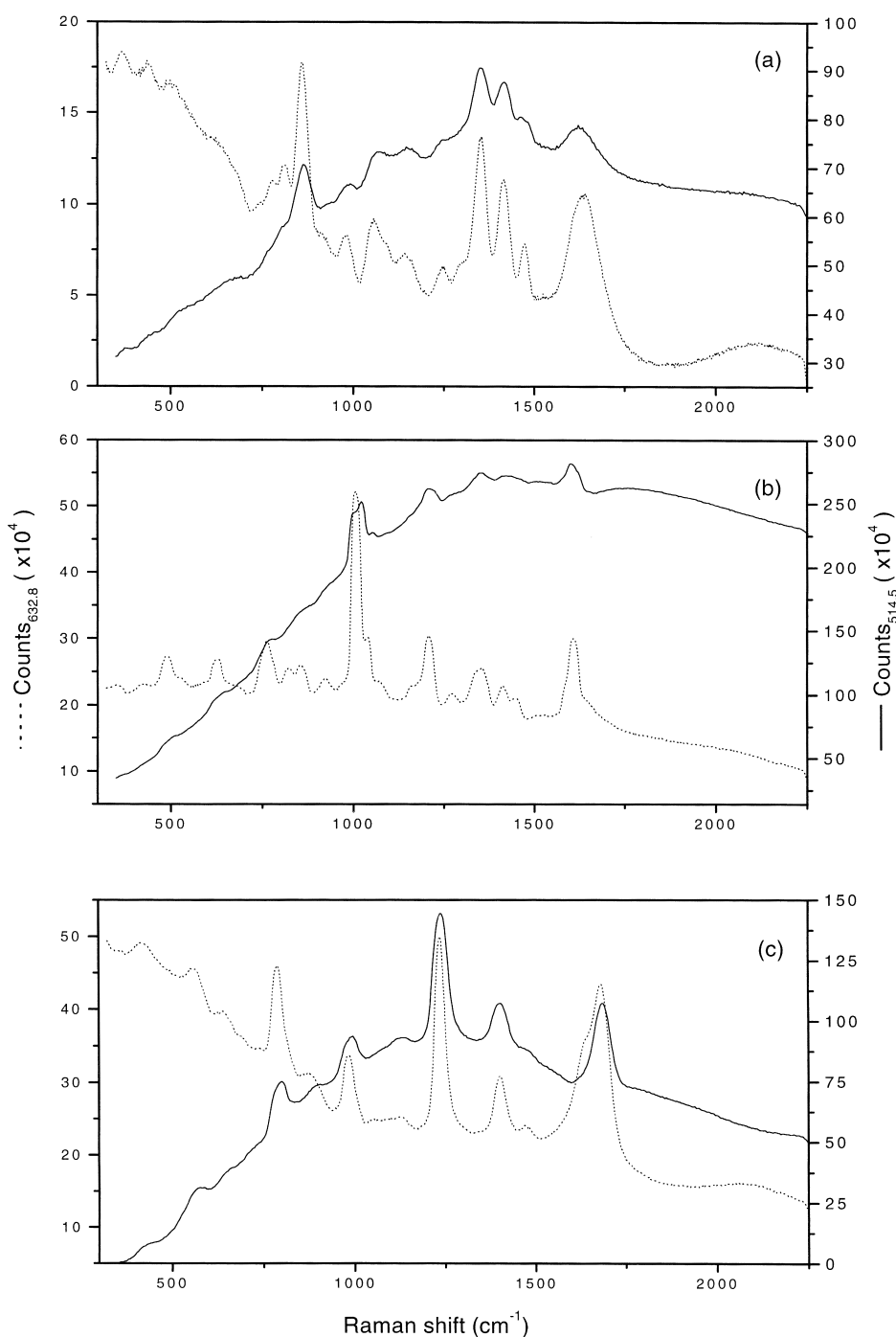


Fig. 2. Background-corrected Raman spectra of (A) phenylalanine, (B) DL-serine and (C) UMP dissolved in water at the 10-mg/ml level. Left-hand axis and dotted curve: excitation wavelength 632.8 nm. Right-hand axis and straight curve: excitation wavelength 514.5 nm. Exposure time: 1000 accumulations of 100 ms.

vibrations of water plays an important role, especially at long optical path lengths as is the case with an LCW [3,4,16]. This absorption is wavelength-dependent. It leads to a wavelength-dependent component in α_L and α_R and to a possible change of the Raman spectrum, which will complicate the analyte identification. As a consequence, S also becomes wavelength dependent.

To account for this wavelength influence, α_L and α_R are split in two parts:

$$\begin{aligned}\alpha_L &= \alpha_{\text{wall}} + \alpha_{\text{abs}}^L \\ \alpha_R &= \alpha_{\text{wall}} + \alpha_{\text{abs}}^R\end{aligned}\quad (4)$$

In Eq. (4) α_{wall} describes the attenuation of light caused by the wall imperfections of the LCW and is assumed to be wavelength independent; α_{abs}^L and α_{abs}^R represent the absorption of light through the overtone vibrations of water at, respectively, the excitation and Raman scatter wavelength. As outlined in Appendix A, the final result for S is:

$$S = \ln\left(\frac{\alpha_{\text{wall}} + \alpha_{\text{abs}}^R}{\alpha_{\text{wall}} + \alpha_{\text{abs}}^L}\right) \cdot \frac{1}{\alpha_{\text{abs}}^R - \alpha_{\text{abs}}^L}\quad (5)$$

Table 1 shows the optimum LCW length S for H_2O and $^2\text{H}_2\text{O}$ solutions, calculated for some laser wavelengths commonly used in RS. Both α_{abs} and α_{wall} were taken from the literature [17–19]. For convenience, instead of I_R , the relative enhancement factor, E_{rel} , of the LCW was calculated, with a 1-cm long LCW for which the contribution of α_{wall} and α_{abs} to the Raman signal is negligible as a reference. Of course, in practice α_{wall} will depend on the LCW material quality. Nevertheless, Table 1 gives a fair impression of the LCW characteristics at different wavelengths.

For H_2O solutions, the largest E_{rel} is found at 514.5 nm. At this excitation wavelength, S is ~ 1 m and the enhancement factor of ~ 40 is nearly constant over the whole Raman spectrum ($0\text{--}3500\text{ cm}^{-1}$). In marked contrast, at an excitation wavelength of $1.064\text{ }\mu\text{m}$ S is less than 10 cm; the corresponding E_{rel} is ≤ 2 and changes significantly with the Raman shift. Obviously, the shortest wavelengths give the best results.

In the previous section it was concluded that shifting to longer wavelengths is needed to decrease the background fluorescence and to improve analyte

Table 1
Optimum LCW length, S , and LCW enhancement factor, E_{rel} , calculated for some laser wavelengths commonly used in RS

Laser	Wavelength (nm)	Raman shift (cm^{-1})								
		0			2000			3500		
		α_{abs} ($\times 10^3\text{ cm}^{-1}$)	S^d (cm)	E_{rel}	α_{abs} ($\times 10^3\text{ cm}^{-1}$)	S^d (cm)	E_{rel}	α_{abs} ($\times 10^3\text{ cm}^{-1}$)	S^d (cm)	E_{rel}
<i>H₂O</i>										
Argon	514.5	0.62 ^a	112	41	0.91 ^a	110	41	3.1 ^a	99	36
Doubled Nd:YAG	532	0.67 ^a	111	41	1.9 ^a	104	38	4.2 ^a	94	34
He–Ne	632.8	3.2 ^a	87	32	17 ^b	57	20	22 ^b	52	18
Diode	690	5.4 ^b	73	27	22 ^b	48	17	72 ^b	27	9
Diode	785	26 ^b	29	11	130 ^b	13	5	147 ^b	12	4
Nd:YAG	1064	144	7	2	3234	1	0.3	5847 ^b	1	0.2
<i>²H₂O</i>										
Argon	514.5	0.89 ^c	109	40	0.54 ^c	111	41	0.38 ^c	112	41
Doubled Nd:YAG	532	0.72 ^c	111	41	0.38 ^c	113	42	0.30 ^c	114	42
He–Ne	632.8	0.34 ^c	116	43	0.55 ^c	114	42	–	–	–
Diode	690	0.33 ^c	116	43	0.74 ^c	113	42	–	–	–
Diode	785	0.75 ^c	110	41	–	–	–	–	–	–

^a Ref. [17].

^b Ref. [18], using $\alpha = 4\pi k/\lambda$.

^c Ref. [19].

^d $\alpha_{\text{wall}} = 8.3 \cdot 10^{-3}\text{ cm}^{-1}$; Ref. [16].

detectability; unfortunately we also have to consider that E_{rel} decreases with increasing wavelength. Excitation at 632.8 or 690 nm seems to be a good compromise: it provides a wavelength long enough for substantially reducing the fluorescence background signal and short enough to avoid substantial re-absorption of laser light and Raman signals by H_2O .

In contrast to the results obtained for H_2O , for $^2\text{H}_2\text{O}$ both S and E_{rel} are virtually independent of the laser excitation wavelength (Table 1). This is in line with the fact that for the whole wavelength range considered the absorption caused by $^2\text{H}_2\text{O}$ is only very small. As a consequence, to permit the use of lasers with long-wavelength excitation, one should replace H_2O by $^2\text{H}_2\text{O}$. This holds, for instance, for the 785-nm diode laser where the absorption coefficients in water are as large as $26 \cdot 10^{-3} \text{ cm}^{-1}$ for the laser line and $130 \cdot 10^{-3} \text{ cm}^{-1}$ for the 2000-cm^{-1} Raman light.

The question arises whether such a solvent replacement will also substantially improve the results at 632.8 nm, the optimum wavelength in LC–LCW–RS, as outlined above. To answer this question, the Raman signals of the NO_2 vibration band of 4-nitroaniline ($\sim 1300 \text{ cm}^{-1}$) were measured as a function of the LCW length, which was varied from 10 to 140 cm. The experiments, which were performed in the stopped-flow mode, are presented in Table 2. There is a distinct difference between the H_2O and $^2\text{H}_2\text{O}$ data. The latter are more favorable, the improvement being 28% at an LCW length of 53 cm. Nonetheless, the differences are relatively small, which is in line with the fact that at 632.8 nm in water α_{abs} and α_{wall} are of the same order of magnitude (at a shift of 2000 cm^{-1} , $1.7 \cdot 10^{-2} \text{ cm}^{-1}$

and $8.3 \cdot 10^{-3} \text{ cm}^{-1}$, respectively). Thus, in practice, the use of expensive $^2\text{H}_2\text{O}$ is not really necessary.

3.5. LC–LCW–RS of nucleotides

The nucleotides UMP, GMP and AMP were separated on an end-capped C-18 column, using an aqueous pH 6.0 buffer as eluent (without any organic modifier), and an injection volume of 25 μl . “On-the-fly” Raman spectra were recorded using an exposure time of 1.5 s. Under these conditions, at the 30-mg/ml injection concentration level tested, rather poor Raman spectra could be recorded for UMP and GMP; AMP was not visible at all. To improve the detectability, stopped-flow experiments were performed: at a predetermined delay time after being monitored by the UV detector, the flow in the LCW was stopped by switching a valve between the UV detector and the LCW, so that a Raman spectrum could be recorded over an extended period of time. Using an exposure time of 10 min, Raman spectra could be recorded down to 10 mg/ml of UMP, 15 mg/ml of GMP and 20 mg/ml of AMP. To further enhance the analyte detectability in terms of concentration units, a larger sample volume of 200 μl was injected, and on-column focusing was used. This implies that the analytes are dissolved in a non-eluting solvent, in the situation at hand an aqueous buffer solution of pH 2. At this pH the analytes have a sufficiently high capacity factor to be trapped on the top of the LC column; they are desorbed as soon as the LC run is started after sample introduction. For the nucleotides concerned, injection volumes of 200 μl did not cause significant band broadening.

Fig. 3 shows the chromatogram (top left) recorded with an absorbance detector at 285 nm of a mixture of 1 mg/ml UMP, 1.5 mg/ml GMP and 2 mg/ml AMP using a 200- μl injection and the corresponding Raman spectra, acquired in the stopped flow mode (exposure time, 10 min). The three LC peaks are well separated even though their shapes are far from ideal, most probably because of the absence of organic modifier and the high analyte concentrations. Such a separation suffices for the purpose of the present study, the exploration of the applicability of LC–LCW–RS.

Although it is possible to record the Raman spectra in a single LC run, three separate runs were

Table 2

Signal intensity of the NO_2 vibration of 4-nitroaniline ($\sim 1300 \text{ cm}^{-1}$) as function of the LCW length in H_2O and $^2\text{H}_2\text{O}$

LCW length (cm)	Signal in H_2O ($\times 10^{-3}$ counts)	Signal in $^2\text{H}_2\text{O}$ ($\times 10^{-3}$ counts)	Increase (%)
7.5	5.1	5.7	13
20	5.9	6.8	15
53	8.3	10.7	28
136	13.3	24.7	86

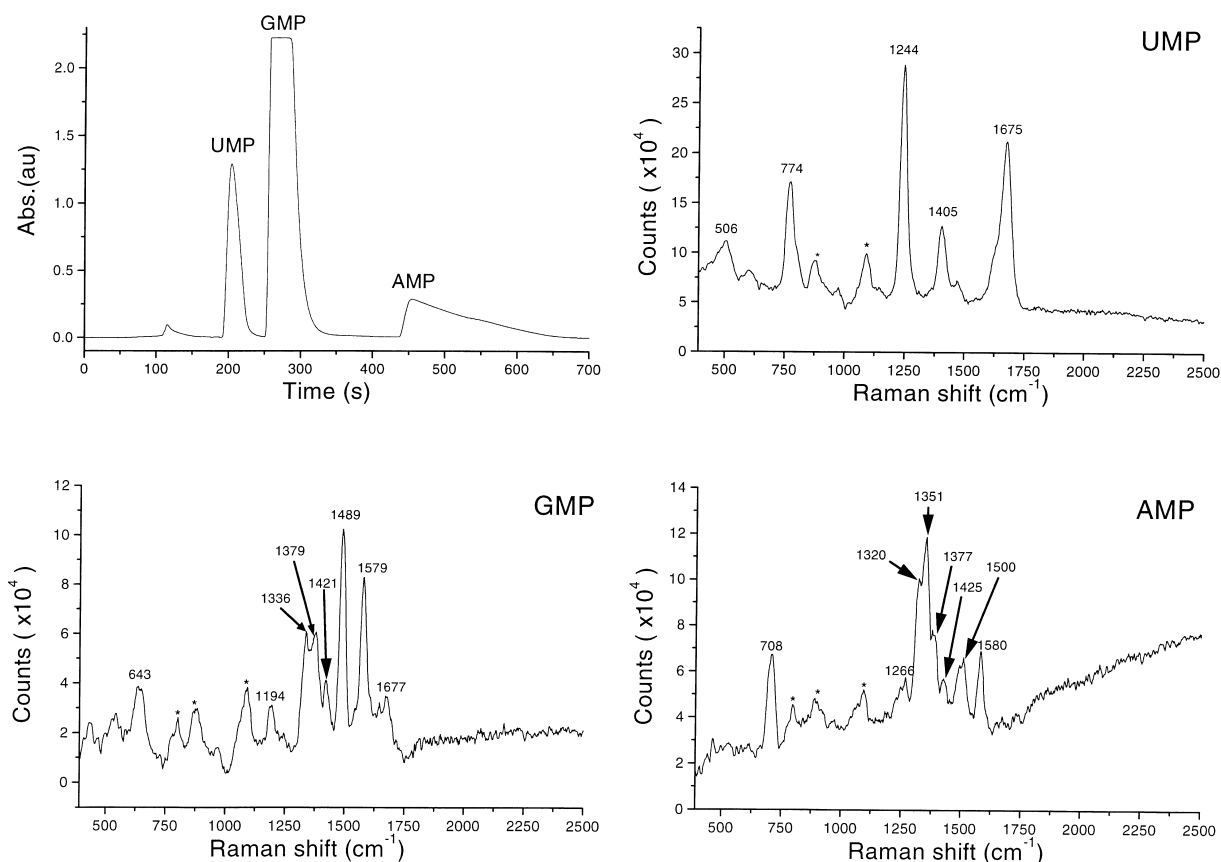


Fig. 3. LC-UV₂₈₅ chromatogram of a mixture of 1 mg/ml UMP, 1.5 mg/ml GMP and 2 mg/ml AMP using aqueous 0.1 M phosphate buffer, pH 6.0, and an injection volume of 200 μ l (top left). Background-corrected Raman spectra acquired in the stopped-flow mode; UMP (top right), GMP (bottom left) and AMP (bottom right). Excitation wavelength: 632.8 nm. Exposure time: 400 accumulations of 1.5 s.

performed, each one focusing on a particular nucleotide. The Raman spectra were background corrected by subtracting the eluent spectrum. Furthermore, they were smoothed using an adjacent 3-point boxcar averaging procedure. The bands marked by an asterisk were also present in the background signal. They are most likely due to non-lasing emission lines of the laser, which were not completely removed by the bandpass filter. Apparently, subtracting of the eluent spectrum did not fully eliminate all background signals.

A complete assignment of the vibration bands in the Raman spectra of the nucleotides is not within the scope of this article, but some remarks should be made. All three nucleotides have a normal vibration

in which the C–C and the C–N bonds of the base residue stretch and contract in phase: the ring breathing vibration of the base residue. This is observed at 774 (785) cm^{-1} for UMP, 643 (671) cm^{-1} for GMP and 708 (730) cm^{-1} for AMP (literature values [20] between brackets). The small differences between the literature and experimental values are presumably due to the relatively low resolution of the spectra ($\sim 21 \text{ cm}^{-1}$) and the lack of calibration points in the low wavenumber range. The three nucleotides have high-frequency ring vibrations at 1244 (1232) and 1405 (1397) cm^{-1} for UMP, 1336 (1325) and 1579 (1578) cm^{-1} for GMP and 1320 (1308), 1351 (1341) and 1580 (1582) cm^{-1} for AMP. The carbonyl group stretching vibrations of

the nucleotide bases UMP and GMP are at 1675 (1681) and 1677 (1686) cm^{-1} , respectively. The weak Raman bands at 1421 (1416) cm^{-1} for GMP and 1425 (1426) cm^{-1} for AMP can be assigned to the methylene scissoring vibrations of the ribose (5'CH₂) group.

The vibration modes of the ribose part are not expected to yield Raman lines as intense as those of the base. Regarding the phosphate group, at $\text{pH} > 7$ it will be present as ROPO_3^{2-} . According to the literature [21], it gives rise to a strong Raman band near 980 cm^{-1} due to the symmetric stretching vibration of the PO_3 group, and a very weak band near 1100 cm^{-1} due to anti-symmetric PO_3 stretching modes. However, under the pH conditions of the LC separation, the phosphate group is predominantly present as $(\text{ROPO}_2\text{OH})^-$ which does not cause any prominent Raman band.

It is obvious from Fig. 3 that the spectra for the nucleotides are sufficiently different to allow their use for identification purposes. The limit of identification (LOI) of the LC–LCW–RS method can be estimated to be 0.1 mg/ml for UMP and 0.5 mg/ml for GMP and AMP.

4. Conclusions

The systematic study on laser and LCW parameters presented above, has led to substantial improvements of the LC–LCW–RS technique. First of all, as far as the laser is concerned, the simple He–Ne laser is an appropriate choice. In order to minimize background fluorescence a laser with a long wavelength, i.e. in the (near) infrared, should be selected. However, at such long wavelengths the (re)-absorption of laser light and Raman signals by the overtone vibrations of water plays an important role. Excitation at 632.8 nm is a good compromise. The optimum LCW length at this wavelength is estimated to be ~ 50 cm. This length is fully compatible with the demands of conventional-size LC; the detector cell volume at this LCW length, and a 220- μm I.D., is only 19 μl . To enable the efficient use of lasers with longer wavelengths — in the literature, 785-nm diode laser excitation is frequently used — H_2O should be replaced by $^2\text{H}_2\text{O}$.

The use of organic modifiers in RPLC seriously

reduces the free spectral window for analyte identification. Therefore LC–LCW–RS separations which do not need organic modifier, such as ion-exchange and size-exclusion LC, are most promising. This implies that — as far as future applicability is concerned — the main area will be bio-analytical chemistry devoted to peptides, proteins, etc., whereas the combination with conventional reversed-phase separations does not have much prospect.

The LOIs of 0.1–0.5 mg/ml obtained for the three nucleotides currently dealt with, are indicative of the state-of-the-art. Further improvements will require efforts especially on the separation side. Optimized LC conditions should result in better peak shapes. In addition, the large-injection-volume approach should be further explored. Finally, it should be evident that it is distinctly worthwhile to develop, next to LC–LCW–RS, LC–resonance RS which can also benefit from the LCW technology.

Appendix A

The increase of the Raman signal in a small segment dx of an LCW in the “forward” mode equals the induced Raman signal in dx minus the losses of the Raman signal already present in dx , or [1]:

$$dI_R = CI \cdot dx - \alpha_R I_R \cdot dx \quad (\text{A1})$$

where I_R is the Raman intensity, C a constant related to the optical configuration, the analyte concentration and the Raman cross-section, and α_R the loss coefficient at the Raman scatter wavelength. The decrease of the laser light intensity, I , as a function of x is given by:

$$I = I_0 e^{-\alpha_L x} \quad (\text{A2})$$

where α_L is the absorption coefficient at the laser wavelength. Combining Eqs. (A1) and (A2) gives:

$$\frac{dI_R}{dx} + \alpha_R I_R = CI_0 e^{-\alpha_L x} \quad (\text{A3})$$

The solution of such a first-order, linear and inhomogeneous differential equation of the form,

$$\frac{dy}{dx} + Cy = Q(x) \quad (\text{A4})$$

is

$$ye^{Cx} = \int Q(x)e^{Cx} dx + C' \quad (\text{A5})$$

Therefore, analogous to Eq. (A5), the solution of Eq. (A3) is

$$I_{\text{R}}e^{\alpha x} = CI_0 \cdot \int e^{(\alpha_{\text{R}} - \alpha_{\text{L}})x} dx + C' \quad (\text{A6})$$

The absorption coefficients should be split in two parts: a wavelength-independent part, α_{wall} , representing the attenuation of light caused by the LCW and a wavelength-dependent part, $\alpha_{\text{abs}}^{\text{R}}$ or $\alpha_{\text{abs}}^{\text{L}}$, representing the absorption of light through the overtone vibrations of water:

$$\begin{aligned} \alpha_{\text{R}} &= \alpha_{\text{wall}} + \alpha_{\text{abs}}^{\text{R}} \\ \alpha_{\text{L}} &= \alpha_{\text{wall}} + \alpha_{\text{abs}}^{\text{L}} \end{aligned} \quad (\text{A7})$$

For the subsequent calculation of the optimum LCW length, S , two situations can be distinguished, a zero Raman shift (in fact representing Rayleigh scattering) and a non-zero Raman shift.

Situation 1: no Raman shift

If there is no Raman shift, the absorption coefficient of the laser light equals that of the scatter light ($\alpha_{\text{L}} = \alpha_{\text{R}}$), and Eq. (A6) simplifies to

$$I_{\text{R}}e^{\alpha_{\text{L}}x} = CI_0 \cdot \int e^0 dx + C' \quad (\text{A8})$$

or

$$I_{\text{R}} = (CI_0x + C')e^{-\alpha_{\text{L}}x} \quad (\text{A9})$$

If it is assumed that for $x=0$, $I_{\text{R}}=0$, Eq. (A9) can be reduced to

$$I_{\text{R}} = CI_0xe^{-\alpha_{\text{L}}x} \quad (\text{A10})$$

The optimum LCW length is obtained if

$$\frac{dI_{\text{R}}}{dx} = 0 \quad (\text{A11})$$

which leads to

$$S = \frac{1}{\alpha_{\text{L}}} \quad (\text{A12})$$

and, consequently, to

$$S = \frac{1}{\alpha_{\text{wall}} + \alpha_{\text{abs}}^{\text{L}}} \quad (\text{A13})$$

Situation 2: a non-zero Raman shift

In this situation α_{L} and α_{R} are not equal and Eq. (A6) needs to be modified:

$$I_{\text{R}} = CI_0e^{-\alpha_{\text{R}}x} \cdot \frac{1}{(\alpha_{\text{R}} - \alpha_{\text{L}})} \cdot e^{(\alpha_{\text{R}} - \alpha_{\text{L}})x} + C''e^{-\alpha_{\text{R}}x} \quad (\text{A14})$$

Using the initial conditions ($x=0$, $I_{\text{R}}=0$) gives:

$$C'' = -\frac{CI_0}{(\alpha_{\text{R}} - \alpha_{\text{L}})} \quad (\text{A15})$$

and Eq. (A14) can be rewritten as:

$$I_{\text{R}} = \frac{CI_0}{(\alpha_{\text{R}} - \alpha_{\text{L}})} \cdot e^{-\alpha_{\text{R}}x} (e^{(\alpha_{\text{R}} - \alpha_{\text{L}})x} - 1) \quad (\text{A16})$$

To calculate S , Eq. (A16) has to be differentiated and set equal to zero:

$$\begin{aligned} \frac{dI_{\text{R}}}{dx} &= \frac{CI_0}{(\alpha_{\text{R}} - \alpha_{\text{L}})} \\ &\cdot [-\alpha_{\text{R}}e^{-\alpha_{\text{R}}x}(e^{(\alpha_{\text{R}} - \alpha_{\text{L}})x} - 1) + e^{-\alpha_{\text{R}}x}(\alpha_{\text{R}} \\ &- \alpha_{\text{L}})e^{(\alpha_{\text{R}} - \alpha_{\text{L}})x}] = 0 \end{aligned} \quad (\text{A17})$$

S is now given by

$$S = \frac{\ln \alpha_{\text{R}} - \ln \alpha_{\text{L}}}{\alpha_{\text{R}} - \alpha_{\text{L}}} \quad (\text{A18})$$

and, after substitution of Eq. (A7), by

$$S = \ln \left(\frac{\alpha_{\text{wall}} + \alpha_{\text{abs}}^{\text{R}}}{\alpha_{\text{wall}} + \alpha_{\text{abs}}^{\text{L}}} \right) \cdot \frac{1}{\alpha_{\text{abs}}^{\text{R}} - \alpha_{\text{abs}}^{\text{L}}} \quad (\text{A19})$$

References

- [1] G.E. Walrafen, Phys. Bl. 30 (1974) 540.
- [2] R. Altkorn, I. Koev, A. Gottlieb, Appl. Spectrosc. 51 (1997) 1554.
- [3] R. Altkorn, I. Koev, R.P. van Duyne, M. Litorja, Appl. Opt. 36 (1997) 8992.
- [4] L. Song, S. Liu, V. Yaskov, M.A. El-Say-Ed, Appl. Spectrosc. 52 (1998) 1364.

- [5] C. Gooijer, G.Ph. Hoornweg, T. de Beer, A. Bader, D.J. van Iperen, U.A.Th. Brinkman, *J. Chromatogr. A* 824 (1998) 1.
- [6] M. Holtz, P.K. Dasgupta, G. Zhang, *Anal. Chem.* 71 (1999) 2934.
- [7] R.J. Dijkstra, A.N. Bader, G.Ph. Hoornweg, U.A.Th. Brinkman, C. Gooijer, *Anal. Chem.* 71 (1999) 4575.
- [8] B.J. Marquardt, P.G. Vahey, R.E. Synovec, L.W. Burgess, *Anal. Chem.* 71 (1999) 4808.
- [9] C.K. Chong, C.K. Mann, T.J. Vickers, *Appl. Spectrosc.* 46 (1992) 249.
- [10] G.W. Somsen, S.K. Coulter, C. Gooijer, N.H. Velthorst, U.A.Th. Brinkman, *Anal. Chim. Acta* 349 (1997) 189.
- [11] R.M. Seifar, R.J. Dijkstra, U.A.Th. Brinkman, C. Gooijer, *Anal. Commun.* 36 (1999) 273.
- [12] R.M. Seifar, M.A.F. Altelaar, R.J. Dijkstra, F. Ariese, U.A.Th. Brinkman, C. Gooijer, *Anal. Chem.* 72 (2000) 5718.
- [13] L.M. Cabalín, A. Rupérez, J.J. Laserna, *Anal. Chim. Acta* 318 (1996) 203.
- [14] <http://webbook.nist.gov/chemistry>
- [15] S.A. Asher, C.R. Johnson, *Science* 225 (1984) 311.
- [16] R. Altkorn, I. Koev, M.J. Pelletier, *Appl. Spectrosc.* 53 (1999) 1169.
- [17] M.R. Querry, P.G. Gary, R.C. Waring, *Appl. Opt.* 17 (1978) 3587.
- [18] L. Kou, D. Labrie, P. Chylek, *Appl. Opt.* 32 (1993) 3531.
- [19] S.A. Sullivan, *J. Opt. Soc. Am.* 53 (1963) 962.
- [20] G.J. Thomas Jr., M. Tsuboi, *Adv. Biophys. Chem.* 3 (1993) 1.
- [21] R.C. Lord, G.J. Thomas Jr., *Spectrochim. Acta* 23A (1967) 2551.